Evolution of Uncorrelated and Correlated Noise in Gaussian and Laplacian Image Pyramids

MARC HENSEL
ROLF-RAINER GRIGAT
Hamburg University of Technology
Institute for Vision Systems
Harburger Schloßstraße 20
21079 Hamburg, GERMANY

BJÖRN EIBEN
Cologne Univ. of Applied Sciences
Inst. of Media and Phototechnology
Betzdorfer Straße 2
50679 Cologne, GERMANY

THOMAS PRALOW
Philips Medical Systems
General X-Ray
Röntgenstraße 24-26
22335 Hamburg, GERMANY

Abstract: Gaussian and Laplacian pyramids are the basis of established image processing applications, for instance, contrast enhancement and noise reduction in medical X-ray imaging. For these techniques to yield optimal results, the noise level at each pyramid scale must be known. So far, however, there is almost no published research regarding this important topic. In this paper, we analyze, to our best knowledge for the first time, noise in pyramids in the spatial domain and show that—and how—noise in Laplacian pyramids depends on the location of a given coefficient. For uncorrelated Gaussian noise we derive mathematical formulations of Gaussian and Laplacian equivalent weighting functions. Correlated noise is addressed by the effect of pyramid operations on autocorrelation functions. The results allow for significant improvement of diverse established methods.

Key–Words: Gaussian pyramid, Laplacian pyramid, equivalent weighting, noise evolution, correlated noise

1 Introduction

Although originally introduced for image compression [3], nowadays Laplacian pyramids are established for a large variety of applications including image transmission, mosaicing, texture analysis, and segmentation. Moreover, pyramids have gained particular importance in medical image processing, for instance, in X-ray image enhancement [4, 11, 12] and noise reduction [8, 9].

For enhancement and noise reduction, an image is decomposed into a Laplacian pyramid, which contains band-pass filtered versions of the original image. The methods operate on Laplacian scales rather than the image and the processed image is reconstructed from the processed pyramid. In order to be optimal, enhancement and noise reduction must be adaptive to the noise level in observed images. This is especially true for medical X-ray imaging, which is characterized by severe noise. As the methods operate on pyramid levels, however, noise *in pyramids* instead of the observed images is required. Unfortunately, and in spite of its importance, to the best knowledge of the authors there is hardly any research published regarding this topic.

This paper is organized as follows: In Chapter 2 we give a short overview of pyramids and multiscale noise evolution. Chapter 3 addresses uncorrelated noise in pyramids by mathematical derivation of Gaussian and Laplacian equivalent weighting functions. In Chapter 4 correlated noise in pyramids is analyzed by means of autocorrelation functions. The paper concludes with a short summary in Chapter 5.

2 State-of-the-Art

As background for the presented work, we give a short introduction to pyramids and related methods to estimate noise in multiscale representations.

2.1 Gaussian and Laplacian Pyramids

Let g denote an observed gray-valued image with intensities $g[m,n] \subset \mathbb{N}_0$ defined at discrete locations $[m,n] \in \Omega = [0, M-1] \times [0, N-1] \subset \mathbb{N}_0^{M \times N}$. An associated *Gaussian pyramid* G with levels (scales) G_k, $k \in [0, K] \subset \mathbb{N}_0$, is a set of different resolutions of g. Starting with $G_0 = g$, the levels G_k, $1 \leq k \leq K$, are created by successive downsampling. In order to reduce aliasing, low-pass filtering is applied prior to decimation. Commonly, both operations are combined in the *Reduce* operation

$$\text{Reduce}(G_k) = (\downarrow 2)\,(h_a * G_k) \tag{1}$$

with linear low-pass filter h_a and downsampling

$$(\downarrow 2)\,(x)[n] = x[2n]\,, \tag{2}$$

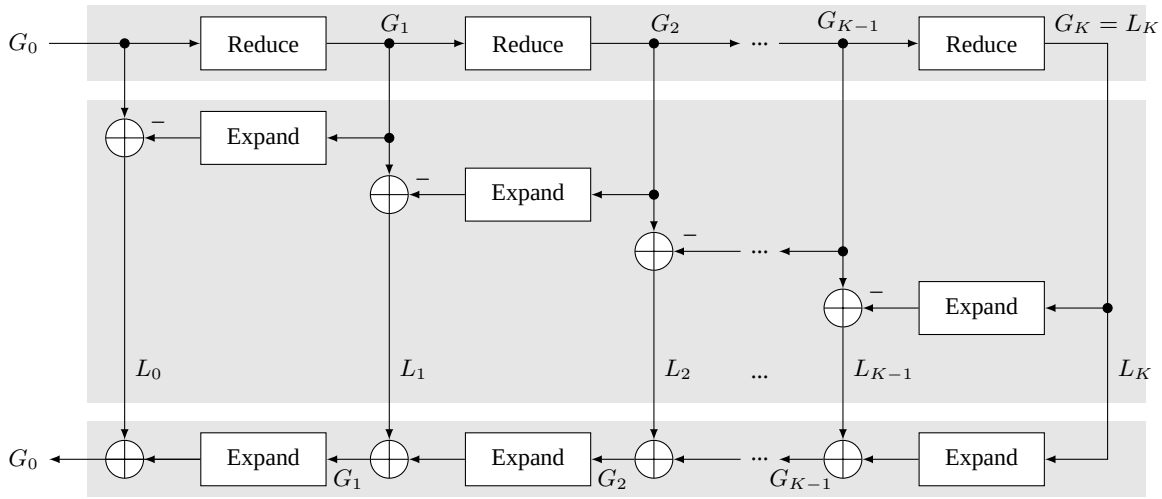

Figure 1: Pyramid creation and reconstruction. A Laplacian pyramid L (middle) is created from the corresponding Gaussian pyramid G (top). Perfect reconstruction yields the original image G_0 (bottom).

which discards every data element with odd index. In 2D data, downsampling is applied in each dimension. With this, the Gaussian pyramid is given by:

$$G_k = \begin{cases} g & : k = 0 \\ \text{Reduce}(G_{k-1}) & : 1 \leq k \leq K \end{cases} \tag{3}$$

Neglecting aliasing, a Gaussian pyramid is a low-pass pyramid and G_k contains the lower $1/2^{dk}$ part of the frequency range of the observed d-dimensional data.

The corresponding *Laplacian pyramid* L with levels L_k contains roughly the frequency components of each G_k lost in the creation of the next higher level G_{k+1}, i.e., the differences between G_k and G_{k+1}. Hence, Laplacian pyramids are band-pass pyramids. Differences $G_k - G_{k+1}$ cannot be calculated directly as G_{k+1} contains less samples than G_k. For this reason, the number of samples in G_{k+1} is increased to match G_k and missing samples are interpolated. Both operations are combined in the *Expand* operation

$$\text{Expand}(G_k) = 2^d h_i * [(\uparrow 2)\, G_k] \tag{4}$$

with data dimension d, linear interpolation filter h_i, and $(\uparrow 2)$ denoting upsampling:

$$(\uparrow 2)\,(x)[n] = \begin{cases} x\left[\frac{n}{2}\right] & : n \text{ even} \\ 0 & : n \text{ odd} \end{cases} \tag{5}$$

Upsampling inserts a zero in-between adjacent data elements. In order to keep the mean image intensity, the result must be multiplied by 2^d. With this, the Laplacian pyramid is defined as follows:

$$L_k = \begin{cases} G_k - \text{Expand}(G_{k+1}) & : 0 \leq k \leq K-1 \\ G_k & : k = K \end{cases} \tag{6}$$

Figure 1 depicts Gaussian and Laplacian pyramid creation and reconstruction. Finally, note that a Laplacian pyramid is a complete representation of g as the corresponding Gaussian pyramid, and hence the original image $g = G_0$, can be reconstructed from L:

$$G_k \overset{(6)}{=} \begin{cases} L_k & : k = K \\ L_k + \text{Expand}(G_{k+1}) & : 0 \leq k \leq K-1 \end{cases} \tag{7}$$

Regardless of the filters h_a and h_i this reconstruction is perfect, i.e., aliasing effects cancel each other out as long as no pyramid level L_k has been modified.

2.2 Multiscale Noise Evolution

In [1], Aach and Kunz derive the noise power spectrum in Laplacian scales L_k in the frequency domain. They note that the result is depending on the pixel grid, i.e., whether sample indices are even or odd, and estimate the noise power spectrum by the average of the grid-dependent spectra.

Further related work estimates noise in wavelet scales rather than pyramid levels. Donoho and Johnstone [5] use the median absolute deviation (MAD) at the finest scale. The method is inaccurate in the presence of structure, though [2]. Yuan and Buckles [14] note that noise decreases with scale and assume noise to dominate at fine scales. They fit a scale-dependent exponential model to noise estimated at low levels. Xu *et al.* [13] evaluate coefficients representing signal-free areas—which, naturally, requires such areas to exist. Finally, Ge and Mirchandani [6] estimate the noise level in a wavelet scale from the adjacent scale making use of $\sigma^2(h * \eta) = \|h\|^2 \sigma^2(\eta)$ for linear filters h and i.i.d. Gaussian noise η. The

prerequisite of independent noise, however, is lost in filtering and, hence, fulfilled *at most* for the lowest scale. In the following, we chose a similar approach, though, without violating above prerequisite.

3 Uncorrelated Noise

We base our analysis on the additive noise model with zero-mean Gaussian noise η—which is valid for a large variety of applications, for instance, medical X-ray imaging [8]. That is, the intensity at location $[m, n]$ in an observed image g is given by $g[m, n] = s[m, n] + \eta[m, n]$ with uncorrupted signal s and zero-mean Gaussian noise η. However, as pyramids are linear, we can neglect s and restrict the analysis to $g = \eta$ where g can take positive and negative values. In the following we assume the noise variance $\sigma^2 = \mathrm{E}\left[(\eta - \mathrm{E}[\eta])^2\right]$ to be known *a priori*, for instance, by using an appropriate noise estimator. Moreover, in this chapter we assume noise to be uncorrelated, i.e., g is a 2-dimensional random field X of independent zero-mean normally-distributed random variables $X[m, n]$ with $[m, n] \in \Omega$.

3.1 Gaussian Pyramid

We address noise in Gaussian pyramid levels G_k by a concept known as *equivalent weighting functions* (EWF) introduced by Burt and Adelson [3]. The underlying idea is that, due to properties of Reduce and Expand operations (1) and (4), a coefficient $G_k[m, n]$ is, in essence, a weighted sum

$$G_k[m, n] = \sum_i \sum_j c_{ij}\, G_0[i, j] \tag{8}$$

of samples of the original image G_0.

If all constants $c_{ij} \in \mathbb{R}_0^+$ were known, we could compute noise variance in G_k directly from the known variance in G_0. To do so, we make use of the weighted sum of Gaussian random variables X_i, for which the variance is given by:

$$\begin{aligned}&\mathrm{var}\left(\sum_{i=0}^{N-1} c_i X_i\right)\\ &= \sum_{i=0}^{N-1} c_i^2 \,\mathrm{var}\,(X_i) + 2\sum_{i=0}^{N-1}\sum_{j=i+1}^{N-1} c_i c_j \,\mathrm{cov}\,(X_i, X_j)\end{aligned} \tag{9}$$

Under the assumptions of independent noise, i.e., $\mathrm{cov}\,(X_i, X_j) = 0$ for $i \neq j$, and identical noise characteristics $\mathrm{var}\,(X_i) = \sigma_0^2$, Equation (9) simplifies to

$$\mathrm{var}\left(\sum_{i=0}^{N-1} c_i X_i\right) = \left(\sum_{i=0}^{N-1} c_i^2\right)\sigma_0^2 = \|\mathbf{c}\|^2\sigma_0^2 \tag{10}$$

with the vector of weights $\mathbf{c} = [c_0, c_1, ..., c_{N-1}]^T$.

Unfortunately, Burt and Adelson merely introduced the concept of EWFs but did not supply mathematical formulations required to evaluate (10). In the following we provide the results of our mathematical derivations. The proofs are omitted due to limited space. They will be handed in later in [7]. However, the lemmas and theorems can be verified, for instance, by drawings and numerical simulations.

To simplify expressions we define a convolution operator similar to sums $\sum$ and products $\prod$ and denote linear convolutions of expressions f_i by:

$$\bigwedge_{i=i_0}^{i_1} f_i = f_{i_0} * f_{i_0+1} * \cdots * f_{i_1} \tag{11}$$

In repeated Reduce operations linear convolution of downsampled data takes place. This is equivalent to downsampling of the original data convolved with an upsampled filter:

Lemma 1 *Let h denote a discrete filter kernel and x discrete signal. Then*

$$\left(h * (\downarrow 2)^k x\right)[n] = \left((\downarrow 2)^k \left((\uparrow 2)^k h * x\right)\right)[n] \tag{12}$$

holds for $k \in \mathbb{N}$.

A compact formulation of EWFs follows from Lemma 1 by a proof by induction:

Theorem 2 *Let G_k, $k \in [0, K]$, be levels of a 1-dimensional Gaussian pyramid G and h_a denote the smoothing filter used for pyramid creation. Level G_k can be calculated from G_0 by*

$$G_k[n] = \left((\downarrow 2)^k (w_{G_k} * G_0)\right)[n]\,, \tag{13}$$

where the equivalent weighting function w_{G_k} for coefficient $G_k[n]$ is given by

$$w_{G_k}[n] = \begin{cases} \delta[n] & : k = 0 \\ \left(\bigwedge_{i=0}^{k-1} (\uparrow 2)^i h_a\right)[n] & : k \geq 1 \end{cases} \tag{14}$$

with unit impulse $\delta[n]$.

Figure 2(a) depicts the typical Gaussian-like shape of EWFs for binomial filters h_a. Finally, we provide functions for 2-dimensional signal:

Theorem 3 *Equivalent weighting functions according to Theorem 2 hold for 2-dimensional signal $G_0[\mathbf{m}]$, $\mathbf{m} = [m, n] \in \Omega$, and yield the dependency*

$$G_k[\mathbf{m}] = \left((\downarrow 2)^k (W_{G_k} * G_0)\right)[\mathbf{m}] \tag{15}$$

with a separable weighting matrix $W_{G_k} = w_{G_k} w_{G_k}^T$.

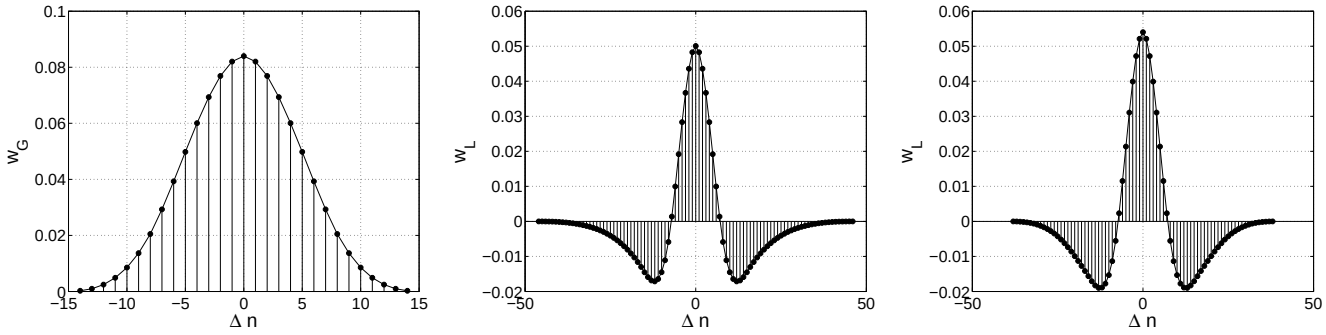

(a) w_{G_3} (b) w_{L_3} (n even) (c) w_{L_3} (n odd)

Figure 2: Equivalent weighting functions (5-tap binomial filters, $k = 3$). (a) Gaussian level G_3. (b) Laplacian level L_3 at even coefficients. (c) Laplacian level L_3 at odd coefficients.

Theorem 3 expresses, in essence, coefficients in G_k as weighted sums of pixels G_0. The latter fulfill the assumption of independent Gaussian noise. Hence, according to (10) noise in G_k is given by

$$\sigma^2_{G_k} = \left\| w_{G_k} w^T_{G_k} \right\|^2 \sigma^2_{G_0} \,. \tag{16}$$

Our numerical simulations verified (16) and showed that for pyramids created, for instance, by 5×5 binomial filters the approach by Ge and Mirchandani [6] yields relative errors of about 40% and 66% for G_2 and G_3, respectively.

3.2 Laplacian Pyramid

In principle, the concept of EWFs also holds for Laplacian pyramids. However, the derivation of a mapping $L_k = f(G_0)$ yields expressions of structure

$$(\uparrow 2)\,((\downarrow 2)\,x[n]) = \begin{cases} x[n] & : n \text{ even} \\ 0 & : n \text{ odd} \end{cases} , \tag{17}$$

i.e., coefficients at even and odd positions in the grid must be distinguished.

Because of limited space and as the approach is similar to the Gaussian case, we merely state the results of our analysis—beginning with 1D signal:

Theorem 4 *Let L_k, $k \in [0, K]$, be levels of a 1-dimensional Laplacian pyramid L and h denote the interpolation filter used for pyramid creation. Level L_k can be calculated from G_0 by*

$$L_k[n] = \left((\downarrow 2)^k \, (w_{L_k} * G_0) \right)[n] \,, \tag{18}$$

where the equivalent weighting function w_{L_k} for coefficient $L_k[n]$ is given by

$$w_{L_k}[n] = \left(w_{G_k} - \left((\uparrow 2)^{k+1} \, (2h_{\mathit{down}}) * w_{G_{k+1}} \right) \right)[n] \tag{19}$$

with h_{down} consisting of even or odd coefficients of h, only, for even or odd n, respectively.

Again, the 2D EWFs are based on 1D EWFs, however, four non-separable weighting matrices depending on the location $[m, n]$ result:

Theorem 5 *Equivalent weighting functions according to Theorem 4 hold for 2-dimensional signal $G_0[\mathbf{m}]$, $\mathbf{m} = [m, n] \in \Omega$, and yield the dependency*

$$L_k[\mathbf{m}] = \left((\downarrow 2)^k \, (W_{L_k} * G_0) \right)[\mathbf{m}] \tag{20}$$

with non-separable weighting matrices

$$W_{L_k}[\mathbf{m}] = \left(W_{G_k} - \left((\uparrow 2)^{k+1} \, h_{\mathbf{m}} * W_{G_{k+1}} \right) \right)[\mathbf{m}] \tag{21}$$

and separable 2D filter kernels

$$h_{\mathbf{m}} = ((\uparrow 2)\, h_{\mathit{down},m}) \cdot ((\uparrow 2)\, h_{\mathit{down},n})^T \tag{22}$$

depending on the four combinations of even and odd indices m and n.

Like in the Gaussian case, noise in L_k can be calculated by applying (10) to the EWFs. However, according to Theorems 4 and 5 w_{L_k} differs for odd and even indices.

Figures 2(b) and (c) depict typical shapes of Laplacian EWFs for binomial filters. Finally, Table 1 quantifies noise in pyramid levels L_k, $0 \le k \le 3$, created by 3×3 and 5×5 binomial filters. While noise levels generally depend on the combination of even and odd coefficients, these are very similar for filter sizes ≥ 5. Hence, for practical purposes, the mean noise level of all even and odd combinations of indices m and n is a sufficiently good approximation.

(a) $h_{3\times3}$

k	$\sigma_{L_k}[m_e, n_e]$	$\sigma_{L_k}[m_o, n_o]$	$\sigma_{L_k}[m_{o/e}, n_{e/o}]$
0	80.04	96.07	91.22
1	27.29	34.71	32.26
2	11.98	15.64	14.40
3	5.78	7.60	6.98

(b) $h_{5\times5}$

k	$\sigma_{L_k}[m_e, n_e]$	$\sigma_{L_k}[m_o, n_o]$	$\sigma_{L_k}[m_{o/e}, n_{e/o}]$
0	93.01	95.48	94.37
1	22.40	23.57	23.03
2	9.74	10.31	10.04
3	4.72	5.00	4.87

Table 1: Uncorrelated noise in Laplacian pyramid levels created with 3×3 and 5×5 binomial filters ($\sigma_{G_0} = 100$). Noise levels differ for combinations of even (m_e, n_e) and odd (m_o, n_o) grid locations $[m, n]$.

4 Correlated Noise

In a practical application, noise need not be uncorrelated in G_0—for instance, in medical X-ray imaging: While noise in a X-ray beam is uncorrelated, it is correlated in observed images. This is due to the detectors, where X-ray photons typically evoke multiple light photons that can contribute to different pixels.

In the following we address correlated noise in pyramids by the effect of Reduce and Expand operations on the autocorrelation function of G_0.

4.1 Gaussian Pyramid

For a real-valued discrete wide-sense stationary random process X, the autocorrelation function R_{XX} is defined as

$$R_{XX}[\Delta n] = \sum_n X[n]\, X[n + \Delta n]\,. \qquad (23)$$

Expressing R_{XX} in terms of expected values,

$$R_{XX}[\Delta n] = E\big[X[n]\, X[\tilde{n}]\big] - E\big[X[n]\big]\, E\big[X[\tilde{n}]\big]\,, \qquad (24)$$

with $\tilde{n} = n + \Delta n$, reveals that at the origin R_{XX} equals the variance of X:

$$R_{XX}[0] = E\big[X[n]^2\big] - E\big[X[n]\big]^2 = \sigma_X^2 \qquad (25)$$

In other words, provided $R_{G_kG_k}$ is known at pyramid scale G_k, the noise level at this scale is determined by $R_{G_kG_k}[0]$. Assume that $R_{G_0G_0}$ of an imaging system is given, for instance, by evaluation of images acquired of a homogeneous scene. We obtain $R_{G_1G_1}$ at the next scale G_1 by analysis of the influence of the Reduce operation (1)—linear filtering followed by downsampling—on $R_{G_0G_0}$. To do so, recall that the autocorrelation function R_{yy} of a linearly filtered signal $y = h * x$ holds [10]

$$R_{yy}[\Delta n] = h[n] * h[-n] * R_{xx}[\Delta n]\,. \qquad (26)$$

For symmetric filters $h[n] = h[-n]$ this expression becomes $R_{yy}[\Delta n] = h * h * R_{xx}[\Delta n]$. Further, it shows that the autocorrelation function of a downsampled signal is the downsampled autocorrelation function of the original signal [10]. Hence, $R_{G_{k+1}G_{k+1}}$, and thus $\sigma_{k+1}^2 = R_{G_{k+1}G_{k+1}}[0]$, is determined by $R_{G_kG_k}$ and the filter h_a used in reduction:

$$R_{G_{k+1}G_{k+1}}[\Delta n] = \left((\downarrow 2)\,(h_a * h_a * R_{G_kG_k})\right)[\Delta n] \qquad (27)$$

Figure 3 depicts $R_{G_0G_0}$ and $R_{L_0L_0}$ for a roughly homogeneous region of a non-clinical X-ray image. Noise is slightly correlated as $R_{G_0G_0}$ does not resemble a unit impulse $\delta[0, 0]$ at the origin as would be the case for uncorrelated noise.

4.2 Laplacian Pyramid

In principle, the evolution of correlated noise in G_0 to Laplacian scales L_k is determined by the same means, i.e., filtered and resampled autocorrelation functions, as in the Gaussian case. A particularity is the usage of different filters in Expand operations (4) at even and odd sample indices according to Theorems 4 and 5.

5 Summary and Conclusion

In the more than two decades since their introduction Gaussian and Laplacian pyramids have become established in a large variety of important image processing applications. Today, they are, inter alia, of outstanding relevance for medical image processing. Astoundingly, however, no means to estimate noise levels in the spatial domain have evolved—although this knowledge can considerably improve, for instance, enhancement and noise reduction by allowing methods to be adaptive to observed noise levels.

In this paper, we provided mathematical formulations for noise levels at arbitrary coefficients in Gaussian and Laplacian pyramids. Inter alia, the analysis of uncorrelated Gaussian noise yielded important insight into the spatial dependency of noise in Laplacian pyramids. This knowledge combined with evolution of noise autocorrelation functions in pyramids

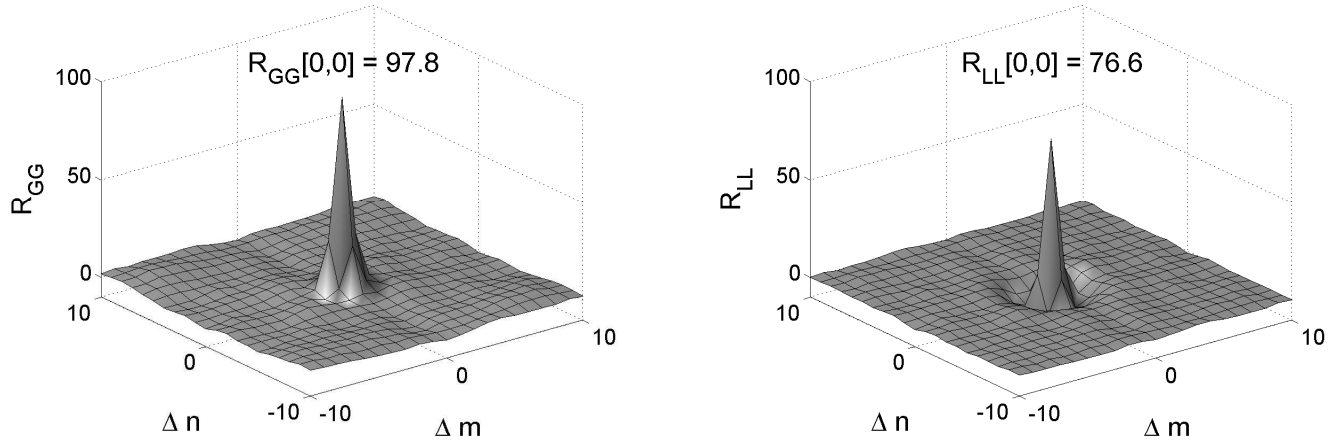

(a) $R_{G_0G_0}$ (b) $R_{L_0L_0}$

Figure 3: Autocorrelation functions of a homogeneous non-clinical X-ray image. Noise is slightly correlated as $R_{G_0G_0}$ is somewhat "smeared". (200×200 regions, σ_0^2 normalized to 100)

allows for scale-dependent—and in case of Laplacian pyramids also spatially dependent—noise estimation in the more general case of correlated noise.

A related state-of-the-art multiscale approach yielded relative errors of about 40% to 66% for uncorrelated noise in practically relevant Gaussian levels and is not applicable for Laplacian pyramids. In contrast, we provide exact solutions for both types of pyramids as well as correlated noise. We expect these results to contribute to a considerable improvement of pyramid-based image processing methods.

Acknowledgments: The authors thank Dietmar Kunz, Cologne University of Applied Sciences, for fruitful discussions.

References:

[1] T. Aach and D. Kunz, Multiscale Linear/Median Hybrid Filters for Noise Reduction in Low Dose X-Ray Images, *Proc. ICIP* 2, 1997, pp. 358–361.

[2] P. Bao and L. Zhang, Noise Reduction for Multiscale Resonance Images via Adaptive Multiscale Products Thresholding, *IEEE Trans. on Medical Imaging* 22, 2003, pp. 1089–1099.

[3] P.J. Burt and E.H. Adelson, The Laplacian Pyramid as a Compact Image Code, *IEEE Trans. on Communications* 31, 1983, pp. 532–540.

[4] S. Dippel, M. Stahl, R. Wiemker, and T. Blaffert, Multiscale Contrast Enhancement for Radiographies: Laplacian Pyramid Versus Fast Wavelet Transform, *IEEE Trans. on Medical Imaging* 21, 2002, pp. 343–353.

[5] D.L. Donoho and I.M. Johnstone, Ideal Spatial Adaptation by Wavelet Shrinkage, *Biometrika* 81, 1994, pp. 425–455.

[6] J. Ge and G. Mirchandani, Softening the Multiscale Product Method for Adaptive Noise Reduction, *Proc. Asilomar Conf. Signals, Systems, Computers*, 2003, pp. 2124–2128.

[7] M. Hensel, Ph.D. thesis, to appear.

[8] M. Hensel, T. Pralow, and R.-R. Grigat, Real-Time Denoising of Medical X-Ray Image Sequences: Three Entirely Different Approaches, *Proc. ICIAR* 2, 2006, pp. 479–490.

[9] D. Kunz, K. Eck, H. Fillbrandt, and T. Aach, A Nonlinear Multi-Resolution Gradient Adaptive Filter for Medical Images, *SPIE Medical Imaging* 5032, 2003, pp. 732–742.

[10] A.V. Oppenheim, R.W. Schafer, and J.R. Buck, *Zeitdiskrete Signalverarbeitung*, 2nd edt., Pearson Studium, 2004.

[11] M. Stahl, T. Aach, and S. Dippel, Digital Radiography Enhancement by Nonlinear Multiscale Processing, *Medical Physics* 27, 2000, pp. 56–65.

[12] P. Vuylsteke and E. Schoeters, Image Processing in Computer Radiography, *CT for Ind. Appl. and Image Proc. in Radiology*, 1999, pp. 87–101.

[13] Y. Xu, J.B. Weaver, D.M. Healy, and J. Lu, Wavelet Transform Domain Filters: A Spatially Selective Noise Filtration Technique, *IEEE Trans. on Image Processing* 3, 1994, pp. 747–758.

[14] X. Yuan and B.P. Buckles, Subband Noise Estimation for Adaptive Wavelet Shrinkage, *Proc. ICPR*, 2004, pp. 885–888.